Crotamiton derivative JM03 extends lifespan and improves oxidative and hypertonic stress resistance in *Caenorhabditis elegans* via inhibiting OSM-9

Keting Bao [1†], Jiali Feng [1†], Wenwen Liu [1†], Zhifan Mao [1], Lingyuan Bao [1], Tianyue Sun [1], Zhouzhi Song [1], Zelan Hu [1*] and Jian Li [1,2,3*]

† Keting Bao, Jiali Feng and Wenwen Liu contributed equally to this work.

* Correspondence: Jian Li (jianli@ecust.edu.cn); Zelan Hu (huzelan@ecust.edu.cn)

[1] State Key Laboratory of Bioreactor Engineering, Frontiers Science Center for Materiobiology and Dynamic Chemistry, Shanghai Key Laboratory of New Drug Design, East China University of Science and Technology, 130 Mei Long Road, Shanghai 200237, China

[2] Yunnan Key Laboratory of Screening and Research on Anti-pathogenic Plant Resources from West Yunnan, College of Pharmacy, Dali University, 5 Xue Ren Road, Dali (Yunnan) 671000, China

[3] Clinical Medicine Scientific and Technical Innovation Center, Shanghai Tenth People's Hospital, Tongji University School of Medicine, Shanghai 200092, China

Abstract

While screening our in-house 1,072 marketed drugs for their ability to extend the lifespan using *Caenorhabditis elegans* (*C. elegans*) as an animal model, crotamiton (*N*-ethyl-o-crotonotoluidide) showed anti-aging activity and was selected for further structural optimization. After replacing the ortho-methyl of crotamiton with ortho-fluoro, crotamiton derivative JM03 was obtained and showed better activity in terms of lifespan-extension and stress resistance than crotamiton. It was further explored that JM03 extended the lifespan of *C. elegans* through osmotic avoidance abnormal-9 (OSM-9). Besides, JM03 improves the ability of nematode to resist oxidative stress and hypertonic stress through OSM-9, but not osm-9/capsaicin receptor related-2 (OCR-2). Then the inhibition of OSM-9 by JM03 reduces the aggregation of Q35 in *C. elegans* via upregulating the genes associated with proteostasis. SKN-1 signaling was also found to be activated after JM03 treatment, which might contribute to proteostasis, stress resistance and lifespan extension. In summary, this study explored a new small molecule derived from crotamiton, which has efficient anti-oxidative, anti-hypertonic and anti-aging effects, and could further lead to promising application prospects.

Introduction

In spite the fact that aging is an inevitable process, many efforts have been made to uncover drugs which could delay aging. Numerous aging associated signaling pathways, discovered in *C. elegans*, are found to be conserved in the mammals [1]. Moreover, many compounds, which extended the lifespan of *C. elegans*, also showed anti-aging effects in the mice model. For example, urolithin A was found to prolong the lifespan and normal activity including mobility and pharyngeal pumping in *C. elegans*, and it also improved the exercise capacity in mice with age-related decline of muscle function [2]. Similarly, rapamycin has been also found to increase the lifespan in worms [3], yeast [4] and flies [5], as well as mean and maximum lifespans in mice [6]. Metformin, a first-line drug for type 2 diabetes treatment, has been widely studied to extend the lifespan both in *C. elegans* [7-9] and mice [10,11].

In order to discover novel anti-aging compounds, we screened our in-house 1,072 marketed drugs using *C. elegans* as an animal model for their ability to extend the lifespan. As marketed drugs generally have definite pharmacokinetics and pharmacodynamics properties and are useful for drug repurposing, our research group is focused on searching compounds for drug repurposing. Herein, in this study, the approved drug crotamiton has been found to show anti-aging activity for the first time and was further selected for the structural optimization.

Crotamiton is an inhibitor of TRPV4 (Transient Receptor Potential Vanilloid-4) channels and has been used as anti-scabies and anti-itch agent in humans for nearly 70

years [12]. TRPV subfamily proteins are encoded by five genes in *C. elegans*, including *osm-9* (*osm*otic avoidance abnormal), *ocr-1* (*o*sm-9/*c*apsaicin receptor *r*elated), *ocr-2*, *ocr-3* and *ocr-4* (ref. [13]). Only loss of *osm-9* or *ocr-2* in worms resulted in the lifespan extension [14]. OSM-9 and OCR-2 can form heterotetrameric channels which transduce signals from olfactory, nociceptive, and serotonergic neurons [15-17], however the role of OSM-9 and OCR-2 in the regulation of stress resistance involves different mechanisms [18]. It has been shown in previous studies that the inactivation of OCR-2 extends the L1 Starvation Survival, while null mutations in *osm-9* did not alter L1 starvation survival [19]. *Osm-9* null mutants showed more resistance to oxidative or hypertonic stress than the control worms [20]. Noticeably, it was reported that taurine, an essential amino acid involved in various physiological functions, promoted longevity of *C. elegans* in oxidative stress condition by inhibiting OSM-9 but not OCR-2 (ref. [18]). Taken together, further extensive research is still needed to decipher the downstream signaling pathways after OSM-9 or OCR-2 activation.

With an aim to get a potential anti-ageing tool molecule, structural optimization based on crotamiton led to the identification of JM03. This molecule displayed better activity than crotamiton in terms of the lifespan extension and stress resistance of *C. elegans*. To further decipher the mechanisms of JM03 involved in the anti-aging activity, this study was conducted with special emphasis on its interaction with OSM-9 or OCR-2.

Results

Crotamiton prolongs lifespan of *C. elegans*

To identify candidate anti-aging compounds, we initially performed a phenotypic screening of our in-house 1,072 marketed drugs with 15 worms per concentration (100 μM) using an *C. elegans* model for their ability of lifespan extension (Figure 1-source data 1). Thereafter, 125 drugs which showed up to 10% increase in mean lifespan extension as compared to the controls were selected for the secondary screening with 30 worms per concentration (100 μM) (Figure 1-source data 2). Finally, 10 drugs which showed up to 10% increase in mean lifespan extension were chosen for the third screening with 60 worms per concentration (400 μM, 100 μM and 25 μM), respectively (Figure 1-source data 2). Apart from recently reported verapamil hydrochloride [21] and chlorpropamide [22] listed in our screening results, crotamiton was finally selected as one hit compound with significant effect on *C. elegans* lifespan extension in this study ($P < 0.01$) (Fig. 1a). The toxicity of crotamiton was evaluated by following parameters: (1) The reproductive capacity was not changed in crotamiton-treated worms at 400 μM (Fig. 1b); (2) For the normal human fetal lung fibroblasts cells MRC-5, crotamiton significantly increased its viability at 200 μM and showed no toxicity even up to 400 μM (Fig. 1c).

In order to exclude the fact that the anti-aging effect of crotamiton was due to its anti-scabies activity, two anti-scabies drugs, benzyl benzoate and permethrin, were also examined along with crotamiton in the same experiment. However, both of the compounds failed to extend the worm lifespan (Fig. S1), which indicated that it was

not the anti-scabies activity of crotamiton which led to the lifespan extension. Moreover, crotamiton showed no significant effect on the bacterial growth, which further ascertained that the anti-aging effect is not the result of insufficient food (Fig. S2a).

JM03, the derivative of crotamiton, has better life extension activity in *C. elegans*

Structural optimization of crotamiton was conducted to identify more potent compounds with better anti-aging activity. The synthetic route for compounds JM01-JM15 was shown in Fig.2a. Treatment of the substituted N-ethylaniline with acryloyl chloride derivatives and potassium carbonate in dichloromethane at room temperature resulted in the formation of JM01-JM05, JM10, JM12, JM13, JM15, **9-11** in about 90-98% yield. Then, compounds JM10, JM12, JM15, **9-11** were conveniently hydrolyzed to provide the corresponding acid JM06-JM09, JM11, JM14.

Studies on the relationship between structure and activity (Fig.S3) showed the removal of the methyl group from the *ortho*-position (Crotamiton) to *meta*-position (JM01) led to the minor improvement in the activity for the R1 substituent group at benzene ring. However, moving the methyl group to the *para*-position (JM02) resulted in better activity. Replacing the *ortho*-methyl with *ortho*-fluoro (JM03), chloro (JM04) and bromo (JM05) significantly increased the activity. Additionally, incorporation of the carboxyl (JM06, JM07) on the benzene ring did not increase the activity. Since the introduction of a carboxyl at the terminal of alkenyl of crotamiton (JM08) improved the activity, we conducted additional modification based on the

119 potent compounds JM02 and JM03. Unfortunately, no remarkable increased activity
120 was observed after this step (Fig.S4). Moreover, the movement of the fluoro
121 substituent from the *ortho*-position (JM03) to the *para*-position (JM13) had no effect
122 on the activity. Further adding carboxyl (JM14) or ethoxycarbonyl (JM15) was found
123 to be detrimental. Considering the introduction of fluorine substituents into drugs can
124 enhance biological activity and increase chemical or metabolic stability [23], JM03 was
125 selected for the following study (Fig. 2a). The lifespan of worms treated with JM03
126 increased significantly as compared to those treated with crotamiton (Fig. 2b). It has
127 been reported that aging would lead to slower and uncoordinated body movement in
128 *C. elegans* [24]. Therefore, keeping this in view, we measured the age-dependent muscle
129 deterioration and diminished pharyngeal pumping rate in worms to assess the
130 healthspan of worms treated with JM03. It was found that JM03 did not change the
131 body bend rate of *C. elegans* at different age (Fig. 2c). JM03-treated groups exhibited
132 increased pharyngeal pumping rate at day 9 (Fig. 2d). Additionally, no changed
133 reproductive capacity was observed in JM03-treated worms (Fig. 2e). Similar to
134 crotamiton, JM03 showed no toxicity against MRC-5 cells and increased their
135 viability at 200 and 400 μM (Fig. 2f). Moreover, the anti-aging effect of JM03 is not
136 the result of insufficient food (Fig. S2b).

137 **JM03-induced extension of lifespan depends on OSM-9 in *C. elegans***

138 Crotamiton is an inhibitor of TRPV4 channel [12], which shows similarity to the *C.*
139 *elegans* channels OSM-9 (26% amino acid identity, 44% identity or conservative

change) and OCR-2 (24% identity, 38% identity or conservative change) [25]. In *C. elegans*, lacking of TRPV channel OSM-9 or OCR-2 resulted in the lifespan extension [26]. Therefore, we further performed the lifespan analysis on *osm-9* or *ocr-2* knockdown worms to investigate the mechanism of JM03. As shown in Fig. 3a and 3b, knockdown of *osm-9* or *ocr-2* via RNAi (Fig. 3d and 3e) extended the lifespan of worms compared to the empty vector group. This indicated that TRPV inhibition extended *C. elegans* lifespan. Notably, JM03 failed to extend the lifespan of osm-9 knockdown worms (Fig. 3a), but still extended the lifespan of *ocr-2* knockdown worms (Fig. 3b). Consistently, JM03 was found to be unresponsive to the lifespan of *osm-9(ky10)* mutants (Fig. 3c). These results suggested that OSM-9 not OCR-2, played a leading role in JM03-mediated longevity.

JM03 improves the ability of nematode to resist oxidative and hypertonic stress through OSM-9

It has been previously shown that the loss of OSM-9 enhanced the resistance of nematodes to the oxidative and hypertonic stress [20]. Therefore, we also evaluated the efficacy of JM03 under the oxidative or hypertonic stress condition. As shown in Fig. 4a, the lifespan of *C. elegans* under paraquat-induced oxidative stress condition was significantly increased in JM03-treated group compared with control or crotamiton-treated group. Then, we examined whether the effect of JM03 under oxidative stress condition is mediated via OSM-9 and OCR-2. It was showed that JM03 treatment didn't increase the lifespan *osm-9(ky10)* mutants (Fig. 4b), but

increased the lifespan of *ocr-2(ak47)* mutants under paraquat-induced oxidative stress condition (Fig. 4c), which suggested OSM-9 is required for JM03 to improve the anti-oxidative stress ability.

In addition, the motile time of *C. elegans* under hypertonic stress condition revealed by motility assays was significantly increased in JM03-treated group compared with control or crotamiton-treated group (Fig. 4d). We also examined whether the effect of JM03 under hypertonic stress condition is mediated via OSM-9 and OCR-2. *Osm-9(ky10)* mutants exhibited increased motility and viability upon prolonged exposures to high osmotic environments compared with wild type *N2* (Fig. 4e), while *ocr-2(ak47)* mutants exhibited motility and viability similar to wild type *N2* (Fig. 4f). For o*sm-9(ky10)* mutants, the increased significance of the motile time under hypertonic stress condition is reduced after JM03 treatment (Fig. 4e). But for *ocr-2(ak47)* mutants, JM03 still significantly increased the motile time of *C. elegans* under hypertonic stress condition (Fig. 4f). Taken together, these results suggested that the OSM-9 inhibition by JM03 increased the anti-oxidative and anti-hypertonic stress ability of *C. elegans*.

JM03 reduces the aggregation of Q35 in *C. elegans* via upregulating the genes associated with proteostasis

It has been reported that oxidative [27] and hypertonic [20] stress enhances rapid and widespread protein aggregation and misfolding in *C. elegans*. Here, we investigated the efficacy of JM03 to reduce the aggregation of protein using Q35::YFP, a worm

strain expressing polyglutamine (Q35) containing yellow fluorescent (YFP) protein in their body wall muscle. Q35::YFP is normally fully soluble in the muscles cells of young worms, but undergoes a slow, progressive aggregation as *C. elegans* ages [28]. Here, we observed the anti-hypertonic stress ability of Q35::YFP and wild type worms was similar (Fig. 4g). JM03 significantly increased the motile time of Q35::YFP or wild type worms exposed to 500 mM NaCl, which is consistent with results shown in Fig. 4d. Meanwhile, Q35::YFP aggregation was significantly reduced when treated with JM03 (Fig. 4h), which suggested JM03 reduced the aggregation of protein in *C. elegans*.

To gain a more detailed picture of the genetic expression after JM03 treatment, worms fed with JM03 or DMSO for 10 days were processed for RNA-sequencing to analyze the altered mRNA abundance (Figure 4-source data, NCBI Gene Expression Omnibus, GSE19373). It was reported that the improved proteostasis capacity of the *osm-9* null mutant was due to altered expression of genes encoding components of the proteostasis network (including protein degradation, protein synthesis, protein folding and so on) [20]. Interestingly, these genes that are upregulated in osm-9 null mutant and play known or presumptive roles in proteostasis, were also upregulated in JM03-treated worms (Fig 4i). Taken together, these results supported the notion that JM03 upregulates the genes associated with proteostasis through OSM-9 leading to enhanced proteostasis capacity, which may improve the ability of nematode to resist oxidative stress and hypertonic stress.

JM03 activates the SKN-1 stress response pathway in *C. elegans*

The transcription factors DAF-16 (ref. 29,30) and SKN-1 play important roles in regulating stress resistance, longevity and proteostasis [31,32]. Therefore, we examined the effect of JM03 on DAF-16 and SKN-1 pathway. JM03 prolonged the lifespan of *daf-16(mu86)* null mutant (Fig. S5), suggesting that DAF-16 is not required for JM03-induced lifespan extension. On the contrary, JM03 did not prolonged the lifespan of *skn-1(zu135)* mutants with loss of function mutation in all SKN-1 isoforms [33], indicating that SKN-1 played an essential role in JM03-induced positive effects (Fig. 5a). Given the dependency of the transcription factor SKN-1 in JM03-induced lifespan extension, we further examined our RNAseq dataset to determine whether expression of target genes of SKN-1 might be perturbed by JM03 treatment. We found that *skn-1* and its target genes, such as *gst-4*, *gst-6*, *gst-7*, *gcs-1*, *prdx-3* and *mtl-1* were upregulated by JM03 (Fig. 5b).

Next, we examined the effect of JM03 on the activation of the SKN-1 stress response pathway using a previously described GFP translational reporter fused to the *skn-1* promoter [33, 34]. JM03 treatment significantly increased the intensity of GFP fluorescence driven by the native *skn-1* promoter (*Is007[skn-1::gfp]*) [33] (Fig. 5c). Concurrently, it also significantly increased the transcriptional expression of *skn-1* itself and *skn-1* regulated genes *gst-4*, *gst-6*, *gst-7*, *gcs-1*, *ctl-2*, *prdx-3* or *mtl-1* (Fig. 5d). Subsequently, we also confirmed the increased expression of glutathione S-transferase-4 (*gst-4*), a key downstream target of SKN-1 (ref. 35), based on the GFP

fluorescence signal of *gst-4::gfp* worms (Fig. 5e). In addition, JM03 did not extend the lifespan of *skn-1(zu135)* mutants under oxidative stress condition (Fig. 5f). In conclusion, JM03 prolongs the lifespan and improves stress-resistance ability of *C. elegans* through SKN-1 pathway.

Discussion

Drug repurposing has emerged as an effective approach for the rapid identification and development of pharmaceutical molecules with novel activities against various diseases based on the already known marketed drugs [36]. Herein, we explored the possibility of identifying the potent drugs which could increase the longevity by screening our in-house marketed drugs. Based on the screening of 1,072 marketed drugs using lifespan extension assays in *C. elegans*, crotamiton, which was known as an anti-scabies and anti-itch agent was identified for its property to increase the lifespan. We also proved that the lifespan extension effect of crotamiton was not the result of its anti-scabies activity (Fig. S1) or the change in the nutritional value of the bacteria (Fig. S2). Thereafter, structural optimization of crotamiton led to the identification of a more potential compound JM03, which was found to show better lifespan expansion and stress resistance activity than crotamiton. Various aspects of the mechanistic action of this molecule were further explored in this study.

It has been reported that crotamiton is an inhibitor of human TRPV4 channel [12], which is homologous to OSM-9 and OCR-2 channels in *C. elegans* [13]. Loss of OCR-2 or OSM-9, can result in the lifespan extension in *C. elegans* [26]. In our study, JM03

245 further increased the lifespan for the *ocr-2* knockdown *C. elegans*, but was ineffective
246 for the knockdown or knockout of *osm-9* (Fig. 3), which suggested JM03 selectively
247 acted on OSM-9, not OCR-2. Furthermore, JM03 improved the antioxidant and
248 anti-hyperosmotic stress resistance of wild type worms (Fig. 4a, d). Interestingly,
249 *osm-9* mutants showed enhanced ability to resist oxidative stress and hypertonic stress
250 (Fig. 4b, e), while *ocr-2* mutants didn't (Fig. 4c, f). These results also supported that
251 JM03 selectively acted on OSM-9, not OCR-2. Consistently, JM03 still had
252 significant anti-oxidant and anti-hyperosmotic effects on *ocr-2* mutants (Fig. 4c, f),
253 but not *osm-9* mutants (Fig. 4b, e). It is noted that OSM-9 is not the only mechanism
254 that mediate the anti-hyperosmotic effect of JM03 because JM03 retained a slight
255 effect on osmotic pressure resistance of the *osm-9* mutants.

256 OSM-9 plays major roles in transduction and regulation of signals in several
257 sensory neurons and is important for processes such as volatile chemotaxis and
258 osmotic avoidance [37]. *Osm-9* null mutant was reported to show enhanced survival in
259 hypertonic environments, not due to altered systemic volume regulation or glycerol
260 accumulation and instead may be due to enhanced proteostasis capacity [20].
261 Consistently, JM03 treatment also enhanced proteostasis capacity in *C. elegans*
262 revealed by reduced aggregation of Q35 (Fig. 4h). Besides, the genes associated with
263 proteostasis, that are upregulated in *osm-9* null mutant, were also upregulated in
264 JM03-treated worms revealed by transcriptome analysis (Fig. 4i). Among these genes,
265 the increased expression of *aquaporin-8* (*aqp-8*) in *osm-9(ok1677)* mutant was also
266 reported by a Germany lab [38]. Considering the essential roles of AQP-8 in sustaining

the salt/water balance in various cells types and tissues, the loss/inhibition of *osm-9* might help to maintain the salt/water balance to promote proteostasis during the response to hyperosmotic stress.

To investigate which downstream signaling was activated after OSM-9 inhibition by JM03, two important stress response transcription factors DAF-16 and SKN-1 were examined [27,39,40]. Lifespan analysis showed that JM03 extended the lifespan through SKN-1 (Fig. 5a), but not DAF-16 (Fig. S5). Then our RNA-sequencing and qPCR data both showed the transcriptional expression of *skn-1* itself and *skn-1* regulated genes were significantly increased in JM03-treated worms (Fig. 5b, d). The expression of SKN-1 and GST-4 was confirmed by using GFP translational reporter worms (*skn-1::gfp* and *gst-4::gfp*) (Fig. 5c, e). These results provide the evidence that JM03 activates SKN-1 signaling that regulates longevity, stress resistance and proteostasis. But how JM03 activates SKN-1 signaling after inhibiting OSM-9 remained to be studied.

In conclusion, overall results showed that JM03 increased the lifespan of *C. elegans* by inhibiting OSM-9, and then activated SKN-1, which improved proteostasis, stress resistance and lifespan extension in *C. elegans* (Fig. 6). Since OSM-9 is the homologous to mammal TRPV channels, it's very interesting to examine whether JM03 acts selectively on a certain TRPV subtypes in mice in future studies.

Materials and methods

Strains

C. elegans were kept at 20℃ on the nematode growth media (NGM) with plates seeded with *E. coli* OP50. Strains used in this study were obtained from Caenorhabditis Genetics Center. The *C. elegans* strains used in this study were as follows: wild type Bristol strain *N2*, CX4544 *ocr-2(ak47) IV*, CX10 *osm-9(ky10) IV*, AM140 rmIs132 [unc-54p::Q35::YFP], LG333 *skn-1(zu135) (IV)/nT1[qIs51] (IV;V); ldIs7 [skn-1b/c::GFP]*, CF1038 *daf-16(mu86) (I)*, CL2166 *dvIs19 [gst-4p::GFP::NLS] (III)*, EU31 *skn-1(zu135) (IV)/ nT1[unc-?(n754);let-?] (IV;V)*.

Lifespan analysis

Worms were synchronized with bleaching buffer, followed by the starvation in M9 buffer at the L1 stage for 24 hours. Worms were thereafter transferred to the NGM plates containing the respective compounds at L4 stage. To avoid progeny hatching, 50 μg/mL of 5-Fluorodeoxyuridine (FUdR) was added to the agar plates from day 0 to day 10. From the 10^{th} day of adulthood, all the groups were transferred to the plates without compounds or FUdR treatment until the end of life. During adulthood, worms were counted every day and transferred to the fresh plates every two days. Death was indicated by total cessation of movement in response to gentle mechanical stimulation. The survival curves were generated using GraphPad Prism 8.3.0. The log-rank (Mantel-Cox) test was used to assess the curve significance.

For lifespan screening experiments, 15 worms were cultured on each Petri dish (60 mm in diameter) containing NGM plate [41,42]. 1 Petri dishes in the 1^{st} round screen, 2 Petri dishes in the 2^{nd} round screen, 4 Petri dishes in the 3^{rd} round screen and 8 Petri

309 dishes in the validation of the effect of drugs were used. In lifespan assay of mutant or
310 control worms, more than 100 worms were used for 1 experiment and a least 3
311 independent experiments were performed for biological replication.

312 **RNAi experiment**

313 *E. coli* strain HT115 was used for this assay. The clones used were *osm-9* (B0212.5)
314 and *ocr-2* (T09A12.3). L4440 was used as the vector. Worms fed with the bacteria
315 expressing L4440 or engineered to produce a gene RNAi effect were cultured until the
316 F4 stage. One subset of the worms was confirmed to exhibit the decreased expression
317 of the gene via qPCR. Then, the other subset of worms was synchronized for a
318 lifespan assay on the control and JM03 400 μM treated NGM plates seeded with
319 bacteria either expressing L4440 or engineered to produce a gene RNAi effect.

320 **Bacterial growth assay**

321 A single colony of bacteria was inoculated in the LB media and cultured at 37℃.
322 For plate assay, 30 μL of bacterial culture (OD_{600}=0.12) was transferred to an NGM
323 plate either with or without crotamiton or JM03 at a concentration of 400 μM, and
324 cultured at 20℃. The bacteria were washed off using 1 mL M9 buffer and OD_{600} was
325 measured every 12 h, with M9 buffer as the blank control. OD was assessed using a
326 Hitachi U-2910 spectrometer with a 10-mm quartz cuvette. At least 3 technical and 3
327 biological independent replicates were performed.

328 **Thrashing assay**

329 Wild type worms *N2* were transferred to the NGM plates at L4 stage and incubated
330 with JM03 at the concentration of 400 μM. For the control and JM03 treatment

groups, thrashes were counted on days 3, 8, and 12. Any change in the midbody bending direction was referred to as a thrash. Worms were placed in M9 buffer drop on an NGM plate without OP50 and allowed to adapt for 30 s. Then, the number of thrashes over 30 s were counted.

In thrashing assay, pharyngeal pumping assay and reproductive lifespan assay, more than 15 worms were used for 1 experiment and a least 3 independent experiments were performed for biological replication.

Pharyngeal pumping assay

Wild type worms *N2* were transferred to the NGM plates at L4 stage with JM03. On days 3, 6, 9, and 12, worms were evaluated by quantifying the contractions of the pharynx over a period of 30 s.

Reproductive lifespan assay

Wild type worms *N2* were transferred to 3.5 cm NGM plates individually at L4 stage with or without JM03 at a concentration of 400 μM. They were further moved to a fresh plate each day until 3 consecutive days without the progeny production. After transferring, plates were checked for progeny after 2 days. For each individual, the last day of the live progeny production was determined as the day of reproductive cessation.

Cell culture and viability assay

MRC-5 cells were maintained in MEM medium (Gibco) supplemented with 10% FBS (42F6590K, Gibco), 1% non-essential amino acid solution (BI), 1% sodium pyruvate solution (BI) and 1% Penicillin-Streptomycin (100×) (Yeasen). Thereafter,

353 the cells were cultured at 37°C in an incubator with humidified atmosphere and with 5%
354 CO_2. Cells were periodically checked to be mycoplasma-free using GMyc-PCR
355 Mycoplasma Test Kit (40601ES10, Yeasen, Shanghai, China).

356 For the cell counting kit-8 (CCK-8) assay, MRC-5 cells (1×10^4 cells/well) were
357 seeded in the 96-well culture plates (100 μL/well) for 12 h. Further, different
358 concentrations of test compounds were added to the plates in 100 μL of fresh medium
359 (the total volume was 200 μL, DMSO < 0.1%) and incubated for 72 h. After removal
360 of the cell culture medium, a 10% CCK-8 solution (Targetmol, C0005) in medium
361 was added and re-incubated for 2 h. Then, the absorbance at 450 nm was measured in
362 a microplate reader (Biotek, Vermont, USA). At least 3 technical and 3 biological
363 independent replicates were performed.

364 **Hypertonic stress resistance assay**

365 Worms were transferred to the NGM plates at L4 stage and incubated with JM03 at
366 a concentration of 400 μM for 4 days. Approximately 60 worms were transferred to
367 NGM plates with 500 mM NaCl and their movement (# moving/total) was assessed.
368 Worms were defined as paralyzed if they failed to move forward upon the tail
369 prodding. Survival was measured every two minutes until all the worms were
370 paralyzed. More than 100 worms were used for 1 experiment and a least 3
371 independent experiments were performed for biological replication.

372 **Oxidative stress resistance assay**

373 Worms were transferred to the NGM plates at L4 stage and incubated with JM03 at
374 a concentration of 400 μM for 4 days. Worms were further transferred to the 24-well

plate (6 worms/well) and incubated in M9 buffer containing 10 mM paraquat. Survival was measured every two hours until all the worms were died. More than 70 worms were used for 1 experiment and a least 3 independent experiments were performed for biological replication.

PolyQ aggregation assay

PolyQ aggregation assay was performed using AM140 *C. elegans* expressing polyQ35::YFP fusion protein in muscle cells. Worms were transferred to the NGM plates at L4 stage and incubated with JM03 at a concentration of 400 μM for 4 days. Thereafter, YFP images were taken using a fluorescence microscopy (Nikon Eclipse Ti2) and the polyQ35::YFP aggregates in worms were quantified manually using imageJ software. More than 50 worms were used for 1 experiment and a least 3 independent experiments were performed for biological replication.

Transcriptome analysis by RNA-sequencing

The transcriptome analysis by RNA sequencing was performed according to a previously published method [43]. Wild type worms *N2* were transferred to the NGM plates at the L4 stage and incubated with JM03 at a concentration of 400 μM for 10 days. At the 10^{th} day of adulthood, worms were collected. Total RNAs were extracted using Trizol Reagent (R0016, Beyotime, Shanghai, China). Further assay and analysis were assisted by Majorbio Bio-Pharm Technology Co. Ltd (Shanghai, China) and are shown in Figure 4-source data.

qRT-PCR analysis

Wild type worms *N2* were transferred to the NGM plates at the L4 stage and

397 incubated with JM03 at a concentration of 400 μM for 4 days. Total RNA was
398 extracted from *C. elegans* with a Total RNA Kit II (R6934-01, Omega, USA) and
399 reverse transcribed using Hifair II 1st Strand cDNA Synthesis SuperMix for qPCR
400 (11123ES60, Yeasen, Shanghai, China) in accordance with the manufacturer's
401 instructions. qPCR was performed using Hieff qPCR SYBR® Green Master Mix
402 (11201ES08, Yeasen, Shanghai, China) on a CFX96 quantitative PCR system
403 (Bio-Rad, USA). Data were processed using CFX Maestro 1.0. The primers used are
404 listed as follows: *ama-1*, forward: TGGAACTCTGGAGTCACACC; reverse:
405 CATCCTCCTTCATTGAACGG. *act-1*, forward: ATGTGTGACGACGAGGTTGC;
406 reverse: ACTTGCGGTGAACGATGGATG. *skn-1*, forward:
407 ACAGTGCTTCTCTTCGGTAGC; reverse: GAGACCCATTGGACGGTTGA. *gst-4*,
408 forward: TGCTCAATGTGCCTTACGAG; reverse: AGTTTTTCCAGCGAGTCCAA.
409 *gst-6*, forward: TTTGGCAGTTGTTGAGGAG; reverse:
410 TGGGTAATCTGGACGGTTTG. *gst-7*, forward:
411 AGGACAACAGAATCCCAAAGG; reverse: AGCAAATCCCATCTTCACCAT.
412 *gst-10*, forward: GTCTACCACGTTTTGGATGC; reverse:
413 ACTTTGTCGGCCTTTCTCTT. *gcs-1*, forward: AATCGATTCCTTTGGAGACC;
414 reverse: ATGTTTGCCTCGACAATGTT. *ctl-1*, forward:
415 GCGGATACCGTACTCGTGAT; reverse: GTGGCTGCTCGTAGTTGTGA. *prdx-3*,
416 forward: CTTGACTTCACCTTTGTATGCC; reverse:
417 GGCGATCTTCTTGTTGAAATCA. *mtl-1*, forward:
418 CAAGTGTGACTGCAAAAACAAG; reverse: GCAGTACTTCTCACAACACTTG.

419 *osm-9*, forward: GACCGCGTAGGAGTACATGG; reverse:
420 GAGAGGTGTGGAAGGCGAAA. *ocr-2*, forward: GCCAGTCAGCTTACCAACAC;
421 reverse: GGTGCAGAATTTGGCGAACG.

422 **SKN-1 and GST-4 expression determination**

423 CL2166 (*gst-4p*::GFP) and LG333 (*skn-1b/c*::GFP) transgenic strains were
424 transferred to the NGM plates at L4 stage and incubated with 400 μM JM03 for 4
425 days. The SKN-1 and GST-4 expression was determined by the fluorescence
426 microscopy (Nikon Eclipse Ti2). The fluorescence intensity was quantified using the
427 ImageJ software. More than 50 worms were used for 1 experiment and a least 3
428 independent experiments were performed for biological replication.

429 **Statistical analysis**

430 All the data are represented as mean ± SD. Statistical analysis was conducted using
431 Graphpad Prism 8.3.0 and significant differences within treatments were determined
432 by Log-rank (Mantel-Cox) test, two-way ANOVA or Student's t-test. $P \leq 0.05$ was
433 considered statistically significant.

434 **General information of Crotamiton derivatives**

435 All the reagents were purchased from commercial corporation without further
436 purification. Nuclear magnetic resonance (NMR) spectroscopy was recorded on 400
437 MHz or 600 MHz Bruker spectrometer at 303 K and referenced to TMS. Chemical
438 shifts were reported in parts per million (ppm, δ). High-resolution mass spectra
439 (HRMS) data were given by Waters LCT or Agilent 6545 Q-TOF. The flash column
440 chromatography was conducted on silica gel (200− 300 mesh) and visualized under

441 UV light at 254 and 365 nm.

442 *General procedures for the synthesis of* ***JM01-JM05, JM10, JM12, JM13, JM15,***

443 ***9-11***

444 To a solution of **1-8** (4.0 mmol) in dichloromethane was added acryloyl chloride

445 derivatives (4.0 mmol) and potassium carbonate (1.66 g, 12.0 mmol) at 0 °C. Then the

446 mixture was stirred at room temperature for about 1 h. After removing the solvent

447 under reduced pressure, the residue was dissolved in ethyl acetate, washed with water

448 and brine. Then the organic phase was dried with sodium sulfate and concentrated *in*

449 *vacuo*. The crude compound was purified by silica gel column chromatography.

450 *(E)-N-ethyl-N-(m-tolyl)but-2-enamide* (**JM01**)

451 780 mg, 96.0 % yield. **^{1}H NMR** (600 MHz, $CDCl_3$) δ 7.33-7.27 (m, 1H), 7.16 (d, J =

452 7.5 Hz, 1H), 6.97 (s, 1H), 6.96 – 6.87 (m, 2H), 5.68 (d, J = 14.8 Hz, 1H), 3.80 (q, J =

453 6.9 Hz, 2H), 2.39 (s, 3H), 1.72 (d, J = 6.7 Hz, 3H), 1.13 (t, J = 7.0 Hz, 3H).

454 ESI-HRMS $[M+H]^+$ calcd for $C_{13}H_{18}NO$: 204.1383, found: 204.1389.

455 *(E)-N-ethyl-N-(p-tolyl)but-2-enamide* (**JM02**)

456 789 mg, 97.0 % yield. **^{1}H NMR** (600 MHz, $CDCl_3$) δ 7.21 (d, J = 7.5 Hz, 2H), 7.03 (d,

457 J = 7.4 Hz, 2H), 6.94 – 6.86 (m, 1H), 5.68 (d, J = 15.0 Hz, 1H), 3.79 (q, J = 7.0 Hz,

458 2H), 2.39 (s, 3H), 1.71 (d, J = 6.7 Hz, 3H), 1.12 (t, J = 7.0 Hz, 3H). ESI-HRMS

459 $[M+H]^+$ calcd for $C_{13}H_{18}NO$: 204.1383, found: 204.1386.

460 *(E)-N-ethyl-N-(2-fluorophenyl)but-2-enamide* (**JM03**)

461 791 mg, 95.4 % yield. **^{1}H NMR** (600 MHz, $CDCl_3$) δ 7.39 – 7.34 (m, 1H), 7.23 – 7.16

462 (m, 3H), 6.99-6.91 (m, 1H), 5.63 (d, J = 15.0 Hz, 1H), 3.87-3.81 (m, 1H), 3.78 – 3.69

(m, 1H), 1.73 (dd, J = 6.9, 1.5 Hz, 3H), 1.12 (t, J = 7.2 Hz, 3H). ESI-HRMS $[M+H]^+$ calcd for $C_{12}H_{15}FNO$: 208.1132, found: 208.1135.

(E)-N-(2-chlorophenyl)-N-ethylbut-2-enamide (**JM04**)

828 mg, 92.5 % yield. **^{1}H NMR** (600 MHz, $CDCl_3$) δ 7.54 – 7.50 (m, 1H), 7.37 – 7.32 (m, 2H), 7.24 – 7.20 (m, 1H), 6.97-6.91 (dq, J = 13.9, 6.9 Hz, 1H), 5.53 – 5.46 (m, 1H), 4.07 (dq, J = 14.3, 7.2 Hz, 1H), 3.48 (dq, J = 14.3, 7.2 Hz, 1H), 1.72 (dd, J = 6.9, 1.6 Hz, 3H), 1.14 (t, J = 7.2 Hz, 3H). ESI-HRMS $[M+H]^+$ calcd for $C_{12}H_{15}ClNO$: 224.0837, found: 224.0804.

(E)-N-(2-bromophenyl)-N-ethylbut-2-enamide (**JM05**)

1009 mg, 94.1 % yield. **^{1}H NMR** (600 MHz, $CDCl_3$) δ 7.70 (dd, J = 8.0, 1.3 Hz, 1H), 7.39 (td, J = 7.6, 1.3 Hz, 1H), 7.28 – 7.25 (m, 1H), 7.22 (dd, J = 7.8, 1.6 Hz, 1H), 6.95 (dq, J = 13.9, 6.9 Hz, 1H), 5.48 (dd, J = 15.0, 1.6 Hz, 1H), 4.14 (dq, J = 14.3, 7.2 Hz, 1H), 3.39 (dq, J = 14.2, 7.2 Hz, 1H), 1.72 (dd, J = 6.9, 1.6 Hz, 3H), 1.15 (t, J = 7.2 Hz, 3H). ESI-HRMS $[M+H]^+$ calcd for $C_{12}H_{15}BrNO$: 268.0332, found: 268.0308.

Ethyl (E)-4-(ethyl(p-tolyl)amino)-4-oxobut-2-enoate (**JM10**)

951 mg, 91.0 % yield. **^{1}H NMR** (600 MHz, $CDCl_3$) δ 7.22 (d, J = 8.0 Hz, 2H), 7.02 (d, J = 8.1 Hz, 2H), 6.82 (q, J = 15.3 Hz, 2H), 4.16 (q, J = 7.1 Hz, 2H), 3.83 (q, J = 7.1 Hz, 2H), 2.39 (s, 3H), 1.24 (t, J = 7.1 Hz, 3H), 1.15 (t, J = 7.1 Hz, 3H). **^{13}C NMR** (150 MHz, $CDCl_3$) δ 165.81, 163.59, 138.29, 138.26, 134.83, 130.71, 130.42, 127.84, 60.92, 44.66, 21.10, 14.10, 12.81. ESI-HRMS $[M+H]^+$ calcd for $C_{15}H_{20}NO_3$: 262.1438, found: 262.1435.

Ethyl (E)-4-(ethyl(2-fluorophenyl)amino)-4-oxobut-2-enoate (**JM12**)

960 mg, 90.5 % yield. **^{1}H NMR** (600 MHz, $CDCl_3$) δ 7.43-7.37 (m, 1H), 7.25 – 7.17 (m, 3H), 6.87 (d, J = 15.2 Hz, 1H), 6.74 (d, J = 15.2 Hz, 1H), 4.16 (q, J = 7.1 Hz, 2H), 3.90 – 3.77 (m, 2H), 1.25 (t, J = 7.1 Hz, 3H), 1.15 (t, J = 7.1 Hz, 3H). ESI-HRMS $[M+H]^+$ calcd for $C_{14}H_{17}FNO_3$: 266.1187, found: 266.1185.

(E)-N-ethyl-N-(4-fluorophenyl)but-2-enamide (**JM13**)

792 mg, 95.5 % yield. **^{1}H NMR** (600 MHz, CDCl3) δ 7.15 – 7.09 (m, 4H), 6.92 (dq, J = 14.0, 6.8 Hz, 1H), 5.62 (d, J = 14.9 Hz, 1H), 3.78 (q, J = 7.1 Hz, 2H), 1.73 (d, J = 6.8 Hz, 3H), 1.13 (t, J = 7.1 Hz, 3H). ESI-HRMS $[M+H]^+$ calcd for $C_{12}H_{15}FNO$: 208.1132, found: 208.1132.

Ethyl (E)-4-(ethyl(4-fluorophenyl)amino)-4-oxobut-2-enoate (**JM15**)

992 mg, 93.5 % yield. **^{1}H NMR** (600 MHz, $CDCl_3$) δ 7.13 (d, J = 6.4 Hz, 4H), 6.84 (d, J = 15.3 Hz, 1H), 6.74 (d, J = 15.3 Hz, 1H), 4.17 (q, J = 7.1 Hz, 2H), 3.83 (q, J = 7.1 Hz, 2H), 1.25 (t, J = 7.1 Hz, 3H), 1.15 (t, J = 7.1 Hz, 3H). ESI-HRMS $[M+Na]^+$ calcd for $C_{14}H_{16}FNO_3Na$: 288.1006, found: 288.1010.

*General procedures for the synthesis of **JM06-JM09, JM11, JM14***

To a solution of **JM10, JM12, JM15, 9-11** (2.0 mmol) in methanol (5 mL) was added 1M NaOH (5 mL). The resulting mixture was stirred at room temperature for 2 h. Then the methanol was removed under reduced pressure, and the residue was acidified to pH = 2 or below with HCl (1M). Then the solution was extracted with ethyl acetate and the combined organic solvents were dried with sodium sulfate and concentrated *in vacuo*. The crude compound was purified by silica gel column chromatography.

(E)-3-(N-ethylbut-2-enamido)-4-methylbenzoic acid (**JM06**)

485 mg, 98.0 % yield. **^{1}H NMR** (600 MHz, $CDCl_3$) δ 10.91 (s, 1H), 8.04 (dd, J = 8.0, 1.3 Hz, 1H), 7.86 (d, J = 1.3 Hz, 1H), 7.43 (d, J = 8.0 Hz, 1H), 7.01 (dq, J = 13.9, 6.9 Hz, 1H), 5.50 (dd, J = 15.0, 1.4 Hz, 1H), 4.11 (dq, J = 14.2, 7.2 Hz, 1H), 3.45 (dq, J = 14.2, 7.2 Hz, 1H), 2.29 (s, 3H), 1.72 (dd, J = 6.9, 1.2 Hz, 3H), 1.18 (t, J = 7.2 Hz, 3H). ESI-HRMS $[M+H]^+$ calcd for $C_{14}H_{18}NO_3$: 248.1281, found: 248.1281.

(E)-4-(N-ethylbut-2-enamido)-3-methylbenzoic acid (**JM07**)

478 mg, 97.0 % yield. **^{1}H NMR** (400 MHz, $CDCl_3$) δ 8.09 (d, J = 1.3 Hz, 1H), 8.02 (d, J = 8.0 Hz, 1H), 7.22 (d, J = 8.1 Hz, 1H), 7.00 (dq, J = 13.8, 6.8 Hz, 1H), 5.49 (d, J = 14.9 Hz, 1H), 4.09 (dq, J = 14.0, 7.1 Hz, 1H), 3.46 (dq, J = 13.9, 7.0 Hz, 1H), 2.28 (s, 3H), 1.72 (d, J = 6.8 Hz, 3H), 1.17 (t, J = 7.1 Hz, 3H). ESI-HRMS $[M+H]^+$ calcd for $C_{13}H_{18}NO$: 248.1281, found: 248.1281.

(E)-4-(ethyl(o-tolyl)amino)-4-oxobut-2-enoic acid (**JM08**)

460 mg, 98.5 % yield. **^{1}H NMR** (600 MHz, $CDCl_3$) δ 7.33 – 7.29 (m, 2H), 7.27 – 7.23 (m, 1H), 7.07 (d, J = 7.6 Hz, 1H), 6.83 (d, J = 15.3 Hz, 1H), 6.65 (d, J = 15.3 Hz, 1H), 4.14 – 4.06 (m, 1H), 3.47 – 3.40 (m, 1H), 2.18 (s, 3H), 1.16 (t, J = 7.2 Hz, 3H). ESI-HRMS $[M+H]^+$ calcd for $C_{13}H_{16}NO_3$: 234.1125, found: 234.1122.

(E)-4-(ethyl(p-tolyl)amino)-4-oxobut-2-enoic acid (**JM09**)

464 mg, 99.5 % yield. **^{1}H NMR** (600 MHz, $CDCl_3$) δ 7.22 (d, J = 7.7 Hz, 2H), 7.00 (d, J = 7.6 Hz, 2H), 6.80 (s, 2H), 3.83 (q, J = 7.1 Hz, 2H), 2.39 (s, 3H), 1.14 (t, J = 7.1 Hz, 3H). **^{13}C NMR** (150 MHz, $CDCl_3$) δ 169.96, 163.42, 138.49, 138.02, 136.52,

130.48, 129.85, 127.75, 44.79, 21.12, 12.75. ESI-HRMS $[M+H]^+$ calcd for $C_{13}H_{16}NO_3^+$: 234.1125, found: 234.1129.

(E)-4-(ethyl(2-fluorophenyl)amino)-4-oxobut-2-enoic acid (**JM11**)

464 mg, 97.8 % yield. **^{1}H NMR** (600 MHz, $CDCl_3$) δ 7.43 – 7.38 (m, 1H), 7.24-7.16 (m, 3H), 6.83 (d, J = 15.2 Hz, 1H), 6.77 (d, J = 15.2 Hz, 1H), 3.89 – 3.76 (m, 2H), 1.15 (t, J = 7.2 Hz, 3H). ESI-HRMS $[M+H]^+$ calcd for $C_{12}H_{13}FNO_3$: 238.0874, found: 238.0874.

(E)-4-(ethyl(4-fluorophenyl)amino)-4-oxobut-2-enoic acid (**JM14**)

471 mg, 99.2 % yield. **^{1}H NMR** (600 MHz, $CDCl_3$) δ 7.13 (d, J = 6.2 Hz, 4H), 6.79 (q, J = 15.3 Hz, 2H), 3.83 (q, J = 6.9 Hz, 2H), 1.15 (t, J = 7.0 Hz, 3H). ESI-HRMS $[M-H]^-$ calcd for $C_{12}H_{11}FNO_3^-$: 236.0728, found: 236.0724.

Acknowledgements

This study was supported by the National Natural Science Foundation of China [22037002, 81772689], the Program for Professor of Special Appointment [Eastern Scholar TP2018025] at Shanghai Institutions of Higher Learning, Sponsored by Natural Science Foundation of Shanghai [21ZR1416700], the Innovation Program of Shanghai Municipal Education Commission [2021-01-07-00-02-E00104], and the Chinese Special Fund for State Key Laboratory of Bioreactor Engineering [2060204].

Conflict of interests

The authors declare no conflicts of interest.

Author Contributions

Research design: KTB, ZLH and JL. Data collection, analysis, and interpretation: KTB, JLF, WWL, ZFM, TYS, ZZS. Preparation of figure composites: KTB, ZLH and JL. Manuscript writing: KTB, ZLH and JL. All authors provided feedback and edits to the manuscript text and approved the final version of the manuscript.

Data Availability Statement

The data used to support the findings of this study are provided as figure source data.

References

1 Kenyon, C. J. The genetics of ageing. *Nature* **464**, 504–512 (2010).

2 Ryu, D. *et al*. Urolithin A induces mitophagy and prolongs lifespan in C. elegans and increases muscle function in rodents. *Nat. Med.* **22**, 879–888 (2016).

3 Robida-Stubbs, S. *et al*. TOR signaling and rapamycin influence longevity by regulating SKN-1/Nrf and DAF-16/FoxO. *Cell Metab.* **15**, 713–724 (2012).

4 Medvedik, O., Lamming, D. W., Kim, K. D. & Sinclair, D. A. MSN2 and MSN4 link calorie restriction and TOR to sirtuin-mediated lifespan extension in Saccharomyces cerevisiae. *PLoS Biol*. **5**, e261 (2007).

5 Bjedov, I. *et al*. Mechanisms of life span extension by rapamycin in the fruit fly Drosophila melanogaster. *Cell Metab*. **11**, 35–46 (2010).

6 Harrison, D. E. *et al*. Rapamycin fed late in life extends lifespan in genetically heterogeneous mice. *Nature* **460**, 392–395 (2009).

7 Cabreiro, F. *et al*. Metformin retards aging in C. elegans by altering microbial folate and methionine metabolism. *Cell* **153**, 228–239 (2013).

8 De Haes, W. *et al*. Metformin promotes lifespan through mitohormesis via the peroxiredoxin PRDX-2. *Proc. Natl. Acad. Sci. USA* **111**, E2501–2509 (2014).

9 Chen, J. *et al*. Metformin extends C. elegans lifespan through lysosomal pathway. *Elife* **6**, e31268 (2017).

10 Anisimov, V. N. *et al*. Metformin slows down aging and extends life span of female SHR mice. *Cell Cycle* **7**, 2769–2773 (2008).

11 Martin-Montalvo, A. *et al*. Metformin improves healthspan and lifespan in mice.

578 *Nat. Commun.* **4**, 2192 (2013).

579 12 Kittaka, H., Yamanoi, Y. & Tominaga, M. Transient receptor potential vanilloid 4

580 (TRPV4) channel as a target of crotamiton and its bimodal effects. *Pflugers Arch*. **469**,

581 1313–1323 (2017).

582 13 Xiao, R. & Xu, X. Z. Function and regulation of TRP family channels in C.

583 elegans. *Pflugers Arch.* **458**, 851–860 (2009).

584 14 Sheng, Y., Tang, L., Kang, L. & Xiao, R. Membrane ion Channels and Receptors

585 in Animal lifespan Modulation. *J. Cell Physiol.* **232**, 2946–2956 (2017).

586 15 Tobin, M. D. *et al*. Combinatorial expression of TRPV channel proteins defines

587 their sensory functions and subcellular localization in C. elegans neurons. *Neuron* **35**,

588 307–318 (2002).

589 16 Ohnishi, K. *et al*. OSM-9 and OCR-2 TRPV channels are accessorial warm

590 receptors in Caenorhabditis elegans temperature acclimatisation. *Sci. Rep.* **10**, 18566

591 (2020).

592 17 Zhang, S., Sokolchik, I., Blanco, G. & Sze, J. Y. Caenorhabditis elegans TRPV

593 ion channel regulates 5HT biosynthesis in chemosensory neurons. *Development* **131**,

594 1629–1638 (2004).

595 18 Moriuchi, M. *et al*. Taurine Inhibits TRPV-Dependent Activity to Overcome

596 Oxidative Stress in Caenorhabditis elegans. *Biol. Pharm. Bull.* **41**, 1672–1677 (2018).

597 19 Lee, B. H. & Ashrafi, K. A TRPV channel modulates C. elegans neurosecretion,

598 larval starvation survival, and adult lifespan. *PLoS Genet.* **4**, e1000213 (2008).

599 20 Lee, E. C. *et al*. Abnormal Osmotic Avoidance Behavior in C. elegans Is

600 Associated with Increased Hypertonic Stress Resistance and Improved Proteostasis.
601 *PLoS One* **11**, e0154156 (2016).
602 21 Liu, W. W. *et al*. Verapamil extends lifespan in Caenorhabditis elegans by
603 inhibiting calcineurin activity and promoting autophagy. *Aging-US*. **12**, 5300–5317
604 (2020).
605 22 Mao, Z. *et al*. Anti-aging effects of chlorpropamide depend on mitochondrial
606 complex-II and the production of mitochondrial reactive oxygen species. *Acta*
607 *Pharmaceutica Sinica B*. https://doi.org/10.1016/j.apsb.2021.08.007.
608 23 Hagmann, W. K. The Many Roles for Fluorine in Medicinal Chemistry. *J. Med.*
609 *Chem.* **51**, 4359–4369 (2008).
610 24 Herndon, L. A. *et al*. Stochastic and genetic factors influence tissue-specific
611 decline in ageing C. elegans. *Nature* **419**, 808–814 (2002).
612 25 Liedtke, W., Tobin, D. M., Bargmann, C. I. & Friedman, J. M. Mammalian
613 TRPV4 (VR-OAC) directs behavioral responses to osmotic and mechanical stimuli in
614 Caenorhabditis elegans. *Proc. Natl. Acad. Sci. USA* **100**, 14531–14536 (2003).
615 26 Riera, C. E. *et al*. TRPV1 pain receptors regulate longevity and metabolism by
616 neuropeptide signaling. *Cell* **157**, 1023–1036 (2014).
617 27 Mark, K. A. *et al*. Vitamin D Promotes Protein Homeostasis and Longevity via
618 the Stress Response Pathway Genes skn-1, ire-1, and xbp-1. *Cell Rep*. **17**, 1227–1237
619 (2016).
620 28 Morley, J. F., Brignull, H. R., Weyers, J. J. & Morimoto, R. I. The threshold for
621 polyglutamine-expansion protein aggregation and cellular toxicity is dynamic and

influenced by aging in Caenorhabditis elegans. *Proc. Natl. Acad. Sci. USA* **99**, 10417–10422 (2002).

29 Baxi, K., Ghavidel, A., Waddell, B., Harkness, T. A. & de Carvalho, C. E. Regulation of Lysosomal Function by the DAF-16 Forkhead Transcription Factor Couples Reproduction to Aging in Caenorhabditis elegans. *Genetics* **207,** 83–101 (2017).

30 Li, S. T. *et al*. DAF-16 stabilizes the aging transcriptome and is activated in mid-aged Caenorhabditis elegans to cope with internal stress. *Aging Cell* **18**, e12896 (2019).

31 Blackwell, T. K., Steinbaugh, M. J., Hourihan, J. M., Ewald, C. Y. & Isik, M. SKN-1/Nrf, stress responses, and aging in Caenorhabditis elegans. *Free Radic. Biol. Med.* **88**, 290–301 (2015).

32 Jones, L. M., Chen, Y. & van Oosten-Hawle, P. Redefining proteostasis transcription factors in organismal stress responses, development, metabolism, and health. *Biol. Chem.* **401**, 1005–1018 (2020).

33 Bishop, N. A. & Guarente, L. Two neurons mediate diet-restriction-induced longevity in C. elegans. *Nature* **447**, 545–549 (2007).

34 Kahn, N. W., Rea, S. L., Moyle, S., Kell, A. & Johnson, T. E. Proteasomal dysfunction activates the transcription factor SKN-1 and produces a selective oxidative-stress response in Caenorhabditis elegans. *Biochem. J.* **409**, 205–213 (2008).

35 Li, H. *et al*. Arginine methylation of SKN-1 promotes oxidative stress resistance

644 in Caenorhabditis elegans. *Redox Biol.* **21**, 101111 (2019).

645 36 Pushpakom, S. *et al*. Drug repurposing: progress, challenges and
646 recommendations. *Nat. Rev. Drug Discov.* **18**, 41–58 (2019).

647 37 Colbert, H. A., Smith, T. L., & Bargmann, C. I. OSM-9, a novel protein with
648 structural similarity to channels, is required for olfaction, mechanosensation, and
649 olfactory adaptation in Caenorhabditis elegans. *J. Neurosci.* **17**, 8259–8269 (1997).

650 38 Igual Gil, C., Jarius, M., von Kries, J. P. & Rohlfing, A. K. Neuronal
651 Chemosensation and Osmotic Stress Response Converge in the Regulation of aqp-8 in
652 C. elegans. *Front. Physiol.* **8**, 380 (2017).

653 39 Alavez, S., Vantipalli, M. C., Zucker, D. J. S., Klang, I. M. & Lithgow, G. J.
654 Amyloid-binding compounds maintain protein homeostasis during ageing and extend
655 lifespan. *Nature* **472**, 226–229 (2011).

656 40 Cohen, E., Bieschke, J., Perciavalle, R. M., Kelly, J. W. & Dillin, A. Opposing
657 Activities Protect Against Age-Onset Proteotoxicity. *Science* **313**, 1604–1610 (2006).

658 41 Petrascheck, M., Ye, X. & Buck, L. B. An antidepressant that extends lifespan in
659 adult Caenorhabditis elegans. *Nature* **450**, 553–556 (2007).

660 42 Evason, K., Huang, C., Yamben, I., Covey, D. F. & Kornfeld, K. Anticonvulsant
661 medications extend worm life-span. *Science* **307**, 258–262 (2005).

662 43 Bao, K. *et al*. Fangchinoline suppresses conjunctival melanoma by directly
663 binding FUBP2 and inhibiting the homologous recombination pathway. *Cell Death*
664 *Dis.* **12**, 380 (2021).

665

Figure Legends

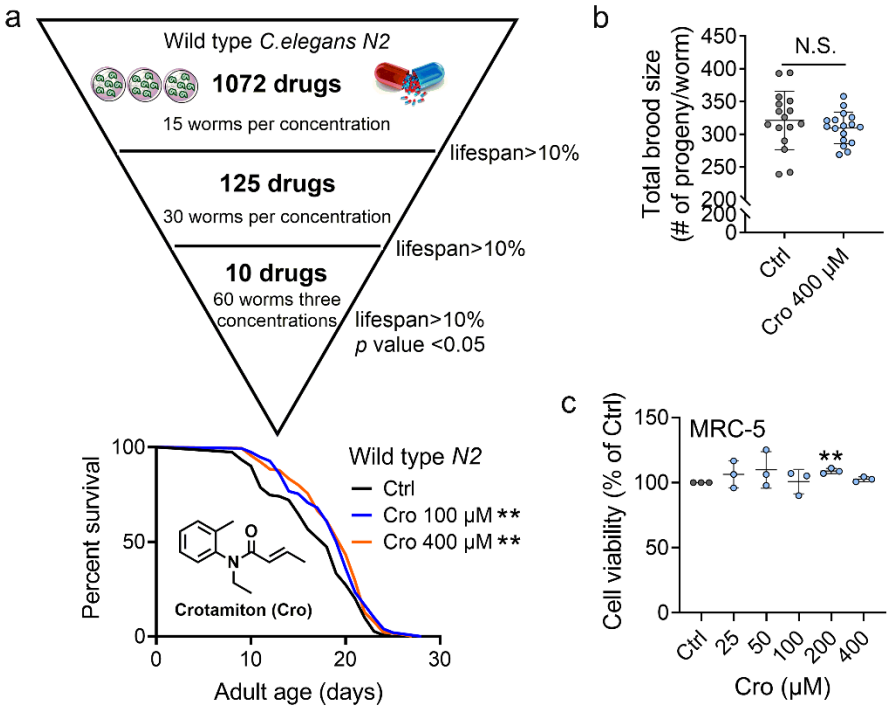

Fig. 1. Crotamiton extends the lifespan of *C. elegans*. (**a**) Phenotypic screening led to the discovery of crotamiton as a hit compound for prolonging the lifespan in wild type (*N2*) worms. Data were compared using the Log-rank test and statistics have been mentioned in Table S1. (**b**) The total brood size of crotamiton-treated *N2* worms. Control n = 16 and crotamiton n = 17. (**c**) The viability of crotamiton-treated MRC-5 cells. *P*-values by Student t-test. $P = 0.0015$ for Cro 200 µM. (**b**, **c**) Data have been represented as the mean ± SD, and comparisons are made using Student t-test. The graphics represent a compilation of at least 3 independent experiments. * $P < 0.05$, ** $P < 0.01$.

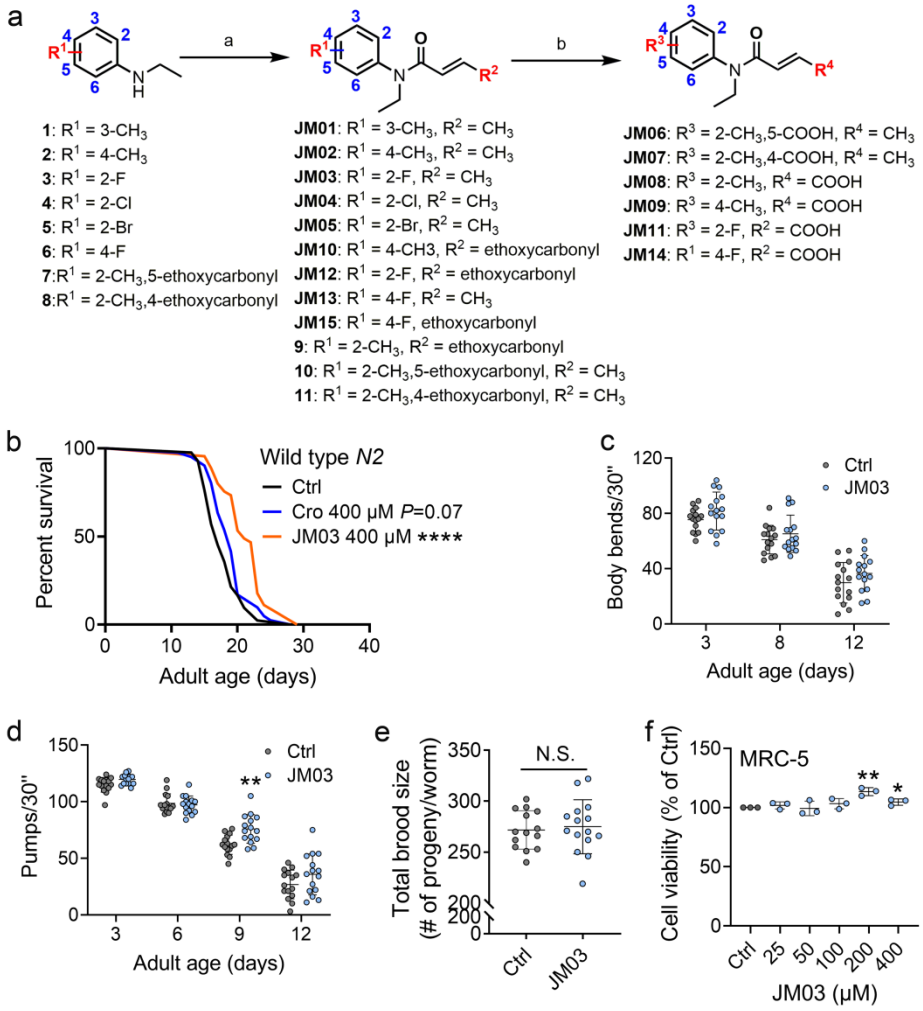

678

679 **Fig. 2. JM03 has better lifespan extension activity in *C. elegans*.** (**a**) Synthesis of
680 compounds JM01−JM15. Reagents and conditions: (a) Acryloyl chloride derivatives,
681 K2CO3, CH2Cl2, 0 °C to rt; (b) 1M NaOH (aq.), CH3OH, rt. (**b**) JM03 prolonged
682 lifespan in wild type (*N2*) worms. Data were compared using the Log-rank test and
683 statistics have been mentioned in Table S1. $P = 0.0737$ for Cro 400 μM. $P < 0.0001$
684 for JM03 400 μM. (**c**) The mobility of JM03-treated *N2* worms by analyzing the body
685 bend rate at day 3, 8 and 12. Control n = 15 and JM03 n = 15. (**d**) The pharyngeal
686 pumping rate of JM03-treated *N2* worms. Control n = 15 and JM03 n = 15 at day 3, 6,
687 9 and 12. *P*-values by two-way AVOVA. $P = 0.0015$ for 9 days. (**e**) The total brood

size of JM03-treated *N2* worms. Control n = 14 and JM03 n = 15. (**f**) The viability of JM03-treated MRC-5 cells. *P*-values by Student t-test. $P = 0.0023$ for JM03 200 µM. $P = 0.0412$ for JM03 400 µM. (**c-d**) Data have been represented as the mean ± SD, and comparisons are made using two-way AVOVA. (**e-f**) Data have been represented as the mean ± SD, and comparisons are made using Student t-test. The graphics represent a compilation of at least 3 independent experiments. * $P < 0.05$, ** $P < 0.01$, **** $P < 0.0001$.

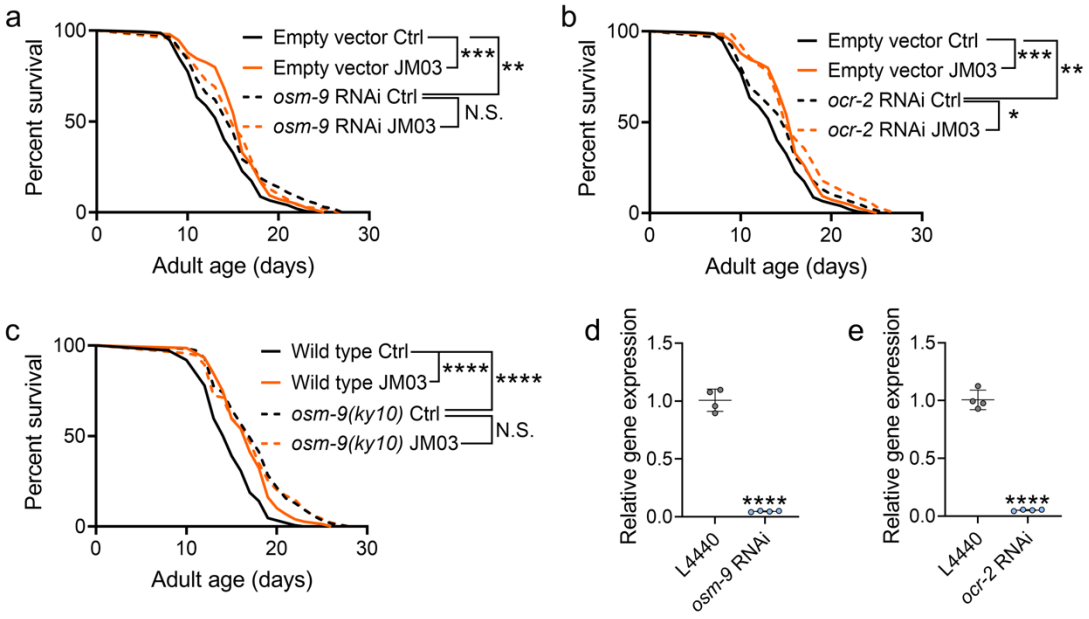

696

697 **Fig. 3. JM03-induced lifespan extension depends on OSM-9.** (**a**) JM03 failed to
698 extend the lifespan of *osm-9* RNAi worms. *P*-values by Log-rank test. $P = 0.0002$
699 between Empty vector Ctrl and Empty vector JM03. $P = 0.0028$ between Empty
700 vector Ctrl and *osm-9* RNAi Ctrl. (**b**) JM03 extended the lifespan of *ocr-2* RNAi
701 worms. *P*-values by Log-rank test. $P = 0.0002$ between Empty vector Ctrl and Empty
702 vector JM03. $P = 0.0084$ between Empty vector Ctrl and *ocr-2* RNAi Ctrl. $P = 0.0259$
703 between *ocr-2* RNAi Ctrl and *ocr-2* RNAi JM03. (**c**) JM03 failed to extend the
704 lifespan of *osm-9(ky10)* mutants. *P*-values by Log-rank test. $P < 0.0001$ for Wild type
705 JM03 and *osm-9(ky10)* Ctrl. (**d**) The transcriptional level of *osm-9* decreased after
706 RNAi treatment. *P*-values by Student t-test. $P < 0.0001$ for *osm-9* RNAi. (**e**) The
707 transcriptional level of *ocr-2* decreased after RNAi treatment. *P*-values by Student
708 t-test. $P < 0.0001$ for *ocr-2* RNAi. (**a-c**) Data are compared using the Log-rank test
709 and statistics have been mentioned in Table S2 and S3. (**d-e**) Data have been
710 represented as the mean ± SD, and comparisons are made using Student t-test. The

711 graphics represent a compilation of at least 3 independent experiments. * $P < 0.05$, **

712 $P < 0.01$, *** $P < 0.001$, **** $P < 0.0001$.

713

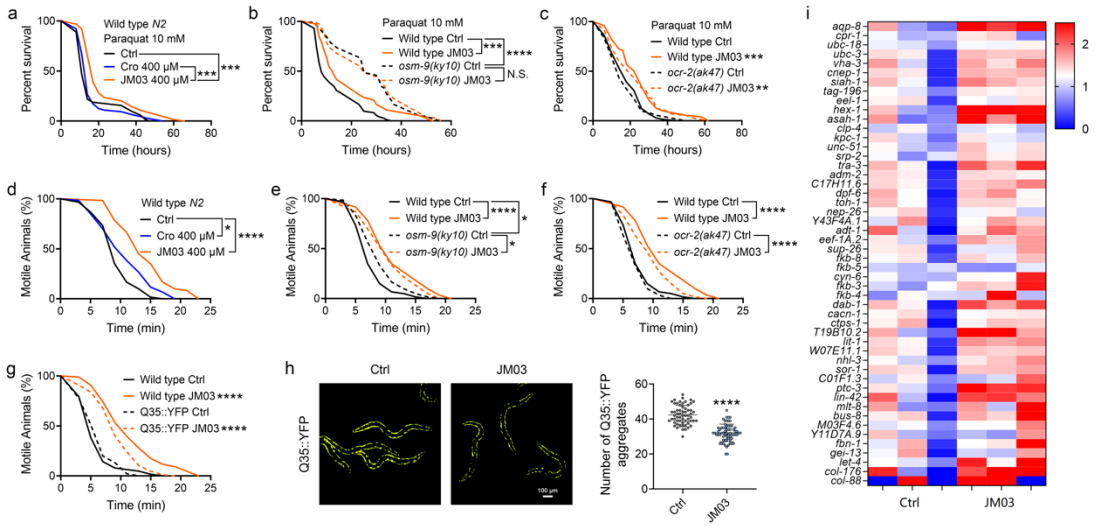

714

715 **Fig. 4. OSM-9 inhibition induced by JM03 has beneficial effect for *C. elegans***
716 **lifespan under oxidative and hypertonic stress conditions.** (**a**) JM03 extended the
717 lifespan of wild type (*N2*) worms under paraquat-induced oxidative stress condition.
718 *P*-values by Log-rank test. $P = 0.0001$ between Ctrl and JM03 400 μM. $P = 0.0002$
719 between Cro 400 μM and JM03 400 μM. (**b**) JM03 failed to extend the lifespan of
720 *osm-9(ky10)* mutants under oxidative stress condition. *P*-values by Log-rank test. $P =$
721 0.0009 between Wild type Ctrl and Wild type JM03. $P < 0.0001$ between Wild type
722 Ctrl and *osm-9(ky10)* Ctrl. (**c**) JM03 extended the lifespan of *ocr-2(ak47)* mutants
723 under oxidative stress condition. *P*-values by Log-rank test. $P = 0.0005$ between Wild
724 type Ctrl and Wild type JM03. $P = 0.0024$ between *ocr-2(ak47)* Ctrl and *ocr-2(ak47)*
725 JM03. (**d**) JM03 significantly reduced the paralysis for wild type worms under
726 NaCl-induced hypertonic stress condition. *P*-values by Log-rank test. $P = 0.0171$
727 between Ctrl and Cro 400 μM. $P < 0.0001$ between Ctrl and JM03 400 μM. (**e**) JM03
728 reduced the responsiveness for *osm-9(ky10)* mutants under hypertonic stress condition.
729 *P*-values by Log-rank test. $P < 0.0001$ between Wild type Ctrl and Wild type JM03. *P*

730 = 0.0128 between Wild type Ctrl and *osm-9(ky10)* Ctrl. P = 0.0254 between
731 *osm-9(ky10)* Ctrl and *osm-9(ky10)* JM03. (**f**) JM03 significantly reduced the paralysis
732 for *ocr-2(ak47)* mutants similar to wild type worms under hypertonic stress condition.
733 P-values by Log-rank test. $P < 0.0001$ between Wild type Ctrl and Wild type JM03. P
734 < 0.0001 between *ocr-2(ak47)* Ctrl and *ocr-2(ak47)* JM03. (**g**) JM03 significantly
735 reduced the paralysis for Q35::YFP worms similar to wild type worms under
736 hypertonic stress condition. P-values by Log-rank test. $P < 0.0001$ between Wild type
737 Ctrl and Wild type JM03. $P < 0.0001$ between Q35::YFP Ctrl and Q35::YFP JM03. (**h**)
738 JM03 significantly reduced the Q35::YFP aggregation. P-values by Student t-test. $P <$
739 0.0001 for JM03 treatment. (**i**) Putative proteostasis genes differentially upregulated
740 by JM03 treatment in wild type worms by transcriptome analysis. (**a**-**g**) Data are
741 compared using the Log-rank test. (**h**) Data have been represented as the mean ± SD,
742 and comparisons are made using Student t-test. The graphics represent a compilation
743 of at least 3 independent experiments. * $P < 0.05$, ** $P < 0.01$, *** $P < 0.001$, **** P
744 < 0.0001.

745

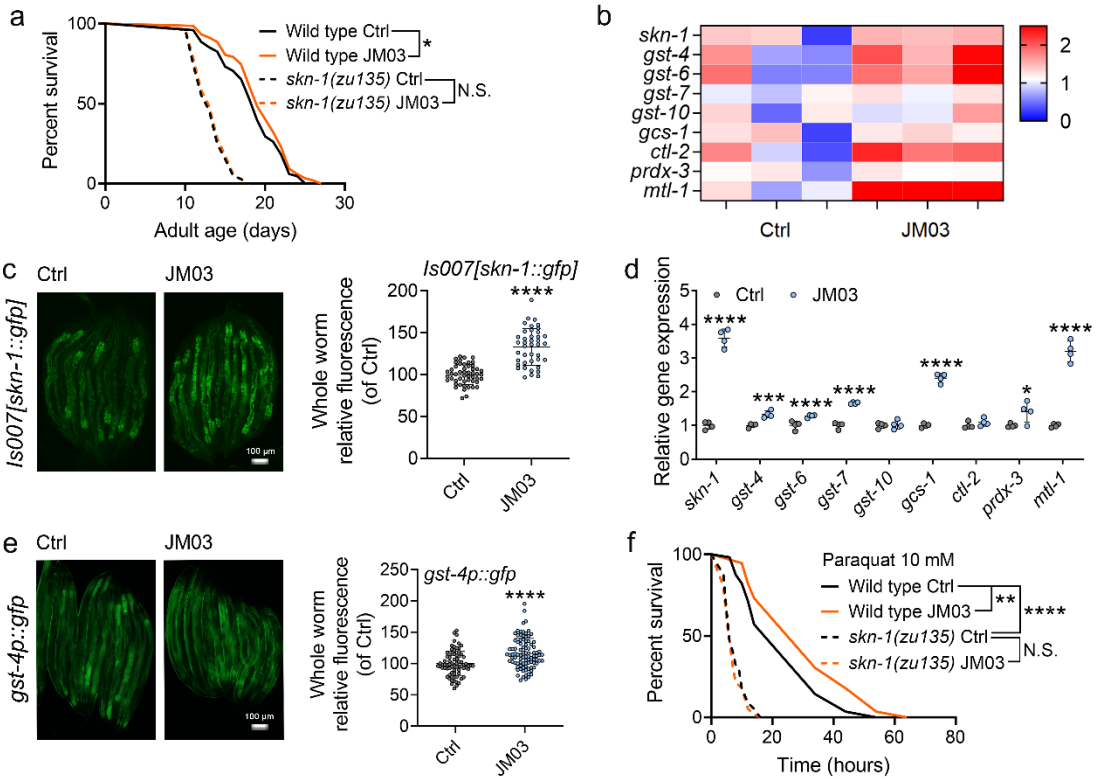

746

747 **Fig. 5. JM03-induced lifespan extension through SKN-1 pathway.** (**a**) JM03
748 treatment failed to extend the lifespan of *skn-1(zu135)* mutants. *P*-values by Log-rank
749 test. $P = 0.0569$ between Wild type Ctrl and Wild type JM03. (**b**) *Skn-1* and its targets
750 genes upregulated by JM03 in wild type worms by transcriptome analysis. (**c**) JM03
751 significantly increased the fluorescence intensity of *skn-1::gfp*. Scale bar = 100 μm.
752 *P*-values by Student t-test. $P < 0.0001$ for JM03 treatment. (**d**) JM03 significantly
753 increased the transcriptional expression of *skn-1* and *skn-1* regulated genes. *P*-values
754 by Student t-test. $P < 0.0001$ for *skn-1*. $P = 0.0006$ for *gst-4*. $P < 0.0001$ for *gst-6*. $P <$
755 0.0001 for *gst-7*. $P < 0.0001$ for *gcs-1*. $P = 0.0424$ for *prdx-3*. $P < 0.0001$ for *mtl-1*. (**e**)
756 JM03 significantly upregulated the fluorescence intensity of *gst-4p::gfp*. Scale bar =
757 100 μm. *P*-values by Student t-test. $P < 0.0001$ for JM03 treatment. (**f**) JM03
758 treatment failed to extend the lifespan of *osm-9(ky10)* and *skn-1(zu135)* mutants under

759 oxidative stress condition. *P*-values by Log-rank test. $P = 0.0059$ between Wild type
760 Ctrl and Wild type JM03. $P < 0.0001$ between Wild type Ctrl and *skn-1(zu135)* Ctrl.
761 (**a**, **f**) Data are compared using the Log-rank test. The graphics represent a compilation
762 of at least 3 independent experiments. (**c**-**e**) Data have been represented as the mean ±
763 SD, and comparisons are made using Student t-test. * $P < 0.05$, ** $P < 0.01$, *** $P <$
764 0.001, **** $P < 0.0001$.

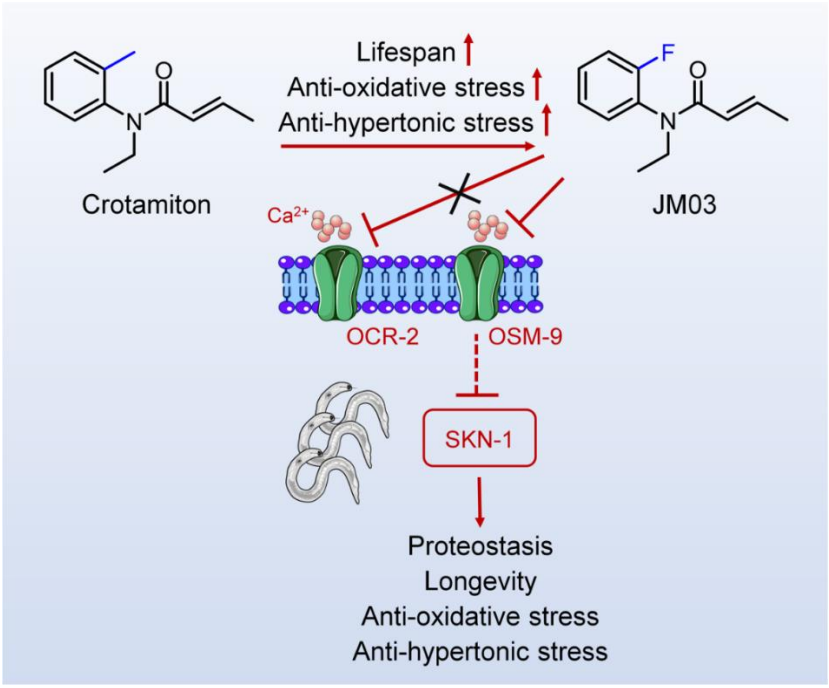

765

766 **Fig. 6. Schematic diagram of the mechanism of action of JM03 for regulating the**
767 **lifespan, anti-oxidative and anti-hypertonic stress ability in *C. elegans*.**

Figure S1.

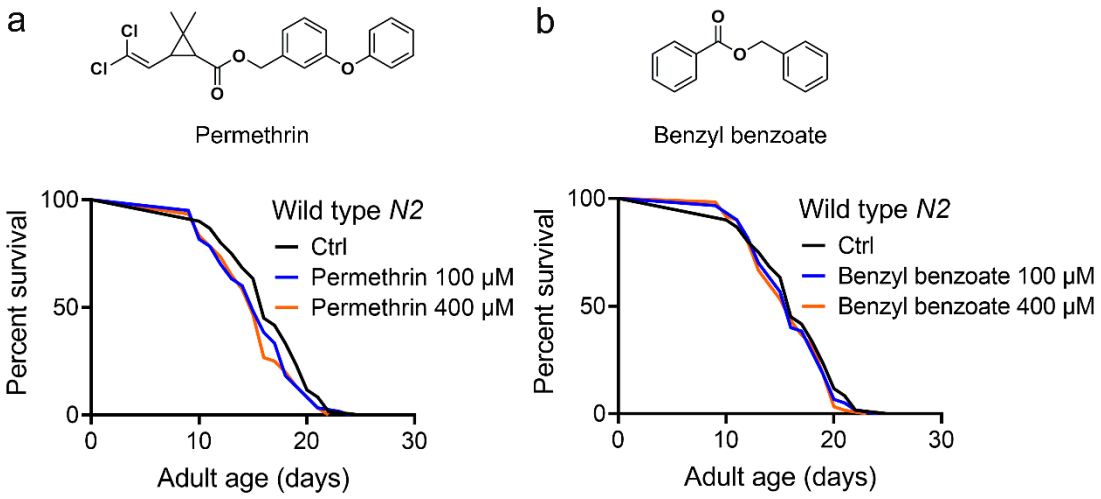

Figure S1. The anti-scabies drugs permethrin and benzyl benzoate failed to extend the lifespan in *C. elegans*. (**a**) Permethrin failed to extend the lifespan of *C. elegans*. (**b**) Benzyl benzoate failed to extend the lifespan of *C. elegans*. (**a**-**b**) Data were compared using the Log-rank test and statistics have been mentioned in Table S1 Experimental group 3. * $P < 0.05$.

Figure S2

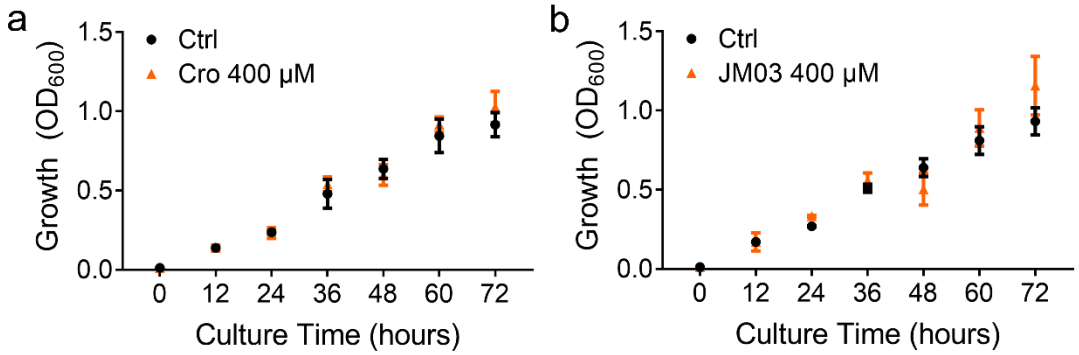

Figure S2. Crotamiton and JM03 did not reduce the bacterial growth at 400 µM concentration. (**a**) Crotamiton did not reduce the bacterial growth at 400 µM concentration. (**b**) JM03 did not reduce the bacterial growth at 400 µM concentration. Data represented as the mean ± SD, and comparisons were made using Student t-test. The graphics represent a compilation of at least 3 independent experiments. * $P < 0.05$.

Figure S3

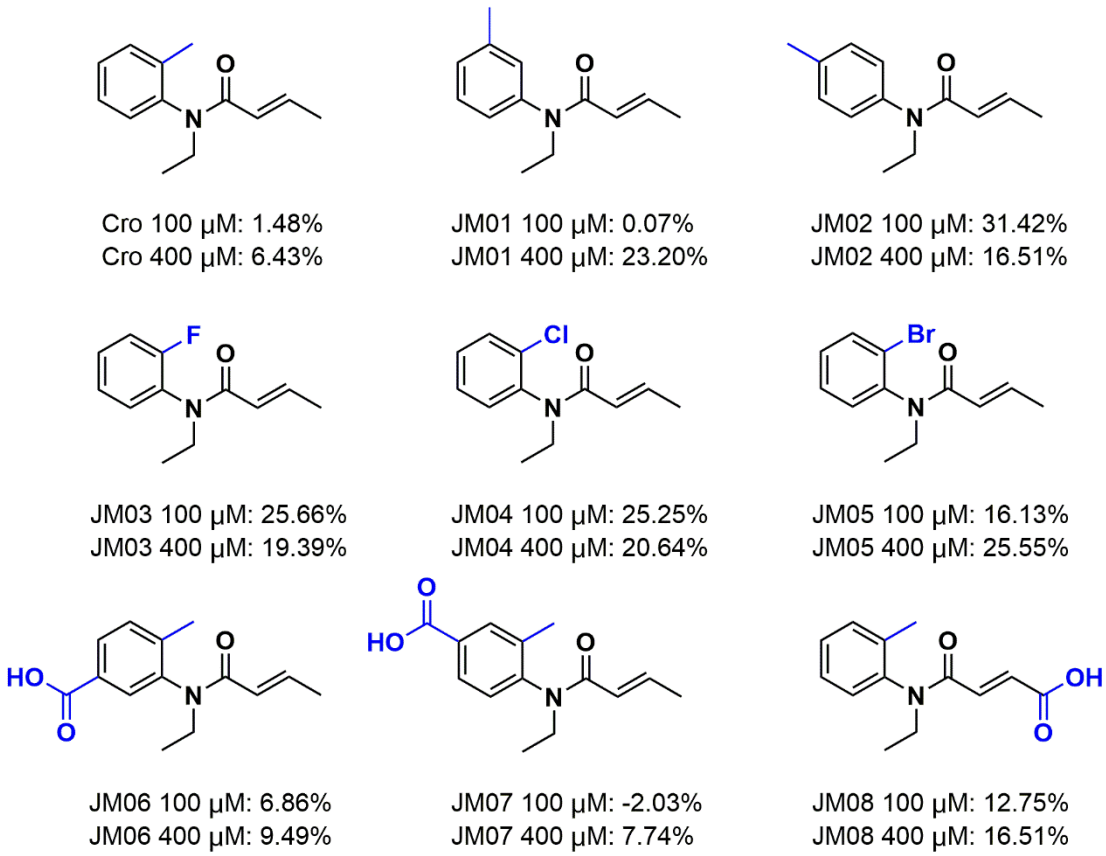

Figure S3. The structures and mean percentage of lifespan extension by crotamiton derivatives.

Figure S4

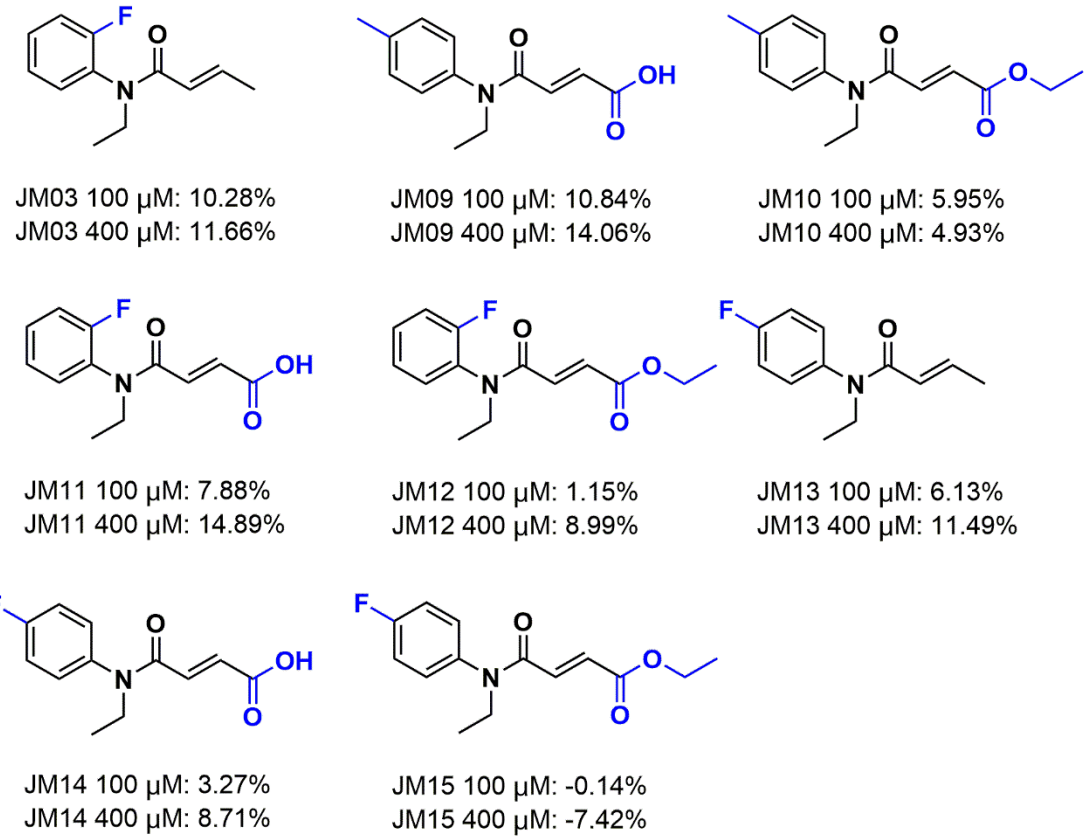

Figure S4. The structures and mean percentage of lifespan extension by crotamiton derivatives.

Figure S5

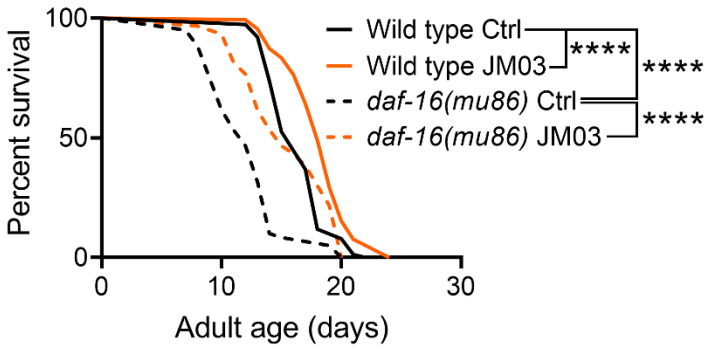

Figure S5. JM03 treatment extended the lifespan of *daf-16(mu86)* mutants. Data are compared using the Log-rank test and statistics have been mentioned in Table S2 Experimental group 2. The graphics represent a compilation of at least 3 independent experiments. ****$P<$ 0.0001.